Bioactive Materials 20 (2023) 194–207

Contents lists available at ScienceDirect

Bioactive Materials

journal homepage: www.keaipublishing.com/en/journals/bioactive-materials

Protein-spatiotemporal partition releasing gradient porous scaffolds and anti-inflammatory and antioxidant regulation remodel tissue engineered anisotropic meniscus

Bingbing Xu [a,b,1], Jing Ye [a,b,1], Bao-Shi Fan [a,b,1], Xinjie Wang [a,b], Ji-Ying Zhang [a,b], Shitang Song [a,b], Yifan Song [a,b], Wen-Bo Jiang [e,**], Xing Wang [c,d,***], Jia-Kuo Yu [a,b,*]

[a] Sports Medicine Department, Beijing Key Laboratory of Sports Injuries, Peking University Third Hospital, No.49, North Garden Road, Haidian District, Beijing 100191, PR China
[b] Peking University Institute of Sports Medicine, No.49, North Garden Road, Haidian District, Beijing 100191, PR China
[c] Beijing National Laboratory for Molecular Sciences, State Key Laboratory of Polymer Physics & Chemistry, Institute of Chemistry, Chinese Academy of Sciences, Beijing, 100190, PR China
[d] University of Chinese Academy of Sciences, Beijing, 100049, PR China
[e] Clinical Translational R&D Center of 3D Printing Technology, Shanghai Ninth People's Hospital, Shanghai Jiao Tong University School of Medicine, Shanghai, 200011, PR China

ARTICLE INFO

Keywords:
Tissue engineering meniscus
Gradient porous scaffolds
Spatiotemporal partition release
Ac2-26 peptide
Anti-inflammatory and anti-oxidant regulation

ABSTRACT

Meniscus is a wedge-shaped fibrocartilaginous tissue, playing important roles in maintaining joint stability and function. Meniscus injuries are difficult to heal and frequently progress into structural breakdown, which then leads to osteoarthritis. Regeneration of heterogeneous tissue engineering meniscus (TEM) continues to be a scientific and translational challenge. The morphology, tissue architecture, mechanical strength, and functional applications of the cultivated TEMs have not been able to meet clinical needs, which may due to the negligent attention on the importance of microenvironment *in vitro* and *in vivo*. Herein, we combined the 3D (three-dimensional)-printed gradient porous scaffolds, spatiotemporal partition release of growth factors, and anti-inflammatory and anti-oxidant microenvironment regulation of Ac2-26 peptide to prepare a versatile meniscus composite scaffold with heterogeneous bionic structures, excellent biomechanical properties and anti-inflammatory and anti-oxidant effects. By observing the results of cell activity and differentiation, and biomechanics under anti-inflammatory and anti-oxidant microenvironments *in vitro*, we explored the effects of anti-inflammatory and anti-oxidant microenvironments on construction of regional and functional heterogeneous TEM via the growth process regulation, with a view to cultivating a high-quality of TEM from bench to bedside.

1. Introduction

As an important heterogeneous structure of the knee joint, the meniscus has important functions such as transmitting and dispersing load, absorbing shock, strengthening proprioception, improving the shape matching of the femur and tibia, lubricating the joint, without which the patient is likely to develop osteoarthritis [1–3]. Tissue engineering meniscus (TEM) strategy is a very promising solution to repair and regenerate damaged meniscus [4]. Studies have shown that there is a big gap between the regenerated meniscus and the natural meniscus [5–7].

In our previous research entitled 'Orchestrated biomechanical,

Peer review under responsibility of KeAi Communications Co., Ltd.
* Corresponding author. Sports Medicine Department, Beijing Key Laboratory of Sports Injuries, Peking University Third Hospital, No.49, North Garden Road, Haidian District, Beijing 100191, PR China.
** Corresponding author.
*** Corresponding author. Beijing National Laboratory for Molecular Sciences, State Key Laboratory of Polymer Physics & Chemistry, Institute of Chemistry, Chinese Academy of Sciences, Beijing 100190, PR China.
E-mail addresses: shjyJiangwenbo@126.com (W.-B. Jiang), wangxing@iccas.ac.cn (X. Wang), yujiakuo@126.com (J.-K. Yu).
[1] These authors have contributed equally to this work.

https://doi.org/10.1016/j.bioactmat.2022.05.019
Received 18 January 2022; Received in revised form 10 May 2022; Accepted 13 May 2022

structural, and biochemical stimuli for engineering anisotropic meniscus', which was published in 2019 in Science Translational Medicine [8]. We applied biomechanical and biochemical stimuli to mesenchymal stem cells seeded into a biomimetic scaffold to induce spatial regulation of fibrochondrocyte differentiation, resulting in physiological anisotropy in the engineered meniscus. Using a customized dynamic tension-compression loading system in conjunction with two growth factors, we induced zonal, layer-specific expression of type I and type II collagens with similar structure and function to those present in the native meniscus tissue. The customized dynamic biomechanical loading system was applied to exert compression-tension strains on the MSC-laden polycaprolactone (PCL) scaffold with regional differences in this research. The biomechanical loading system not only need to be customized, but TEM was susceptible to contamination during compression-tension strains process. Therefore, whether a non-uniform pore 3D printing scaffold could replace the biomechanical stimulation to construct a regional and functional heterogeneous TEM remains to be explored.

The heterogeneous structure of TEM close to the natural meniscus play an important role in the fabrication of meniscus scaffolds. The zonal, layer-specific expression of type I and type II collagens were achieved by means of biomechanical stimulation rather than by the spatiotemporal partition release of two growth factors in our previous research [8]. There have been no research on 3D-printed non-uniform porous TEM scaffolds that can meet clinical needs. The natural meniscus is composed of a heterogeneous group of connective tissue cells [9,10]. 3D printing technology using biodegradable polymers can be used for the regeneration of various tissues or organs [11–14].

The heterogeneous function of scaffolds like natural meniscus are also extremely important in the TEM. Studies have shown that it is necessary to restore the fibrocartilage phenotype during meniscus regeneration in order to obtain a functional meniscus to withstand tensile and compressive stress [12,15]. In addition to restoring cell and matrix properties, the regenerated meniscus tissue should also have certain mechanical functions, similar to efforts to regenerate the heart, kidneys, and bones [16,17]. Meniscus regeneration with heterogeneous tissue properties and function could be achieved through protein-releasing cellular biomaterial scaffolds [18]. If 3D-printed non-uniform porous scaffolds could replace the biomechanical stimulation to construct heterogeneous TEM, our study also explores whether the spatiotemporal partition release of two growth factors using a novel rotation-immersion formulation method could enhance the effect of heterogeneous structure.

Furthermore, with the emphasis on the microenvironment of TEM construction and meniscus regeneration, our research also studied whether better quality TEM construction requires anti-inflammatory and anti-oxidant microenvironment. In tissue engineering strategies, it is necessary to regulate the inflammation existing in the diseased tissues and inflammatory stimuli caused by TEM. Regulating the recruitment of white blood cells and the subsequent steps of the inflammatory process through drug delivery strategies, especially controlling the phenotype of macrophages, has become an important link in the field of tissue engineering. It is extensively described on the phenotypic spectrum of macrophages ranging from traditionally activated pro-inflammatory M1 macrophages to tissue-depositing M2a or anti-inflammatory M2b macrophages [19,20]. How to control the balance of M1-M2 in a reasonable and timely manner during the entire healing process is a key factor in tissue engineering and regenerative medicine applications.In addition to inflammation in diseased tissues, the redox balance of cells and the surrounding microenvironment is also closely related to the physiological functions of tissue regeneration [6]. Providing appropriate antioxidants and improving the oxidative stress environment can promote the TEM regeneration [21–23].

Simultaneously regulating inflammation and redox microenvironment to maintain healthy cell function and prevent oxidative damage will be a new concept to improve quality of TEM regeneration. Tissue engineering composite scaffolds can release a variety of small molecule drugs, growth factors and other biologically active molecules to regulate inflammation and promote tissue growth [24,25], but there are relatively few drugs used for meniscal grafts for knee joint replacement. Among different pro-regression mediators, endogenous annexin A1 can effectively treat inflammatory diseases [26]. Ac2-26 is a peptide derived from the N-terminus of Annexin A1, which has the pharmacological activity of the intact protein [27]. This short peptide is not as specific as enzymes and unlikely to lose the activity during the process of incorporation into materials [28–31]. Ac2-26 peptide can inhibit various aspects of the inflammatory response, such as cell adhesion and transport, thereby reducing the infiltration of neutrophils and monocytes/macrophages, which has strong anti-inflammatory, anti-oxidant and healing effects in the body.

On the basis of our previous research [8], we extend the research. Herein, we prepared and screened a kind of polylactone/4-arm poly (ethylene glycol) hydrogel (PCL@tetra-PEG) composite scaffolds with heterogeneous bionic structure and function, excellent biomechanical properties, anti-inflammatory and anti-oxidant effects. By means of the 3D printing technology, PCL meniscus scaffold was firstly fabricated with a gradient porous and heterogeneous structures. Then, we devised a rotation-immersion formulation in the metal mold to generate the PCL@tetra-PEG meniscus scaffold, in which tetra-PEG hydrogel not only improved biomechanical properties of PCL@tetra-PEG scaffold to match the native meniscus, but also provided opportunities on achieving variously regional encapsulation and spatiotemporal partition release of two human growth factors, exhibiting the multiple tissue phenotype with heterogeneous functions. Notably, the simultaneous encapsulation of Ac2-26 peptide within the composite scaffold could exert the anti-inflammatory and antioxidant effects on regulation of complex microenvironment to promote tissue regeneration. Therefore, we believe this composite scaffold will be developed as a potential meniscus with a view to cultivating a high-quality of TEM from bench to bedside (Fig. 1).

2. Materials and methods

2.1. Study design

The overall objective of the study was to determine whether the synergistic effect of gradient porous scaffolds design, spatiotemporal partition release of growth factors and anti-inflammatory and antioxidant regulation would provide the benefits for heterogeneous meniscus regeneration.

We systematically investigated the efficacy for reconstructing functional anisotropic meniscus *in vitro*, including the following: (i) Properties of different molecular weight meniscus scaffold compositing hydrogel; (ii) ECM synthesis and gene expression of COL-1, and COL-2, as the primary macromolecules in the native meniscus and (iii) fibrochondrogenic differentiation of MSCs under the synergistic effect of gradient porous scaffolds design, spatiotemporal partition release of growth factors and anti-inflammatory and antioxidant regulation.

2.2. Fabrication of 3D-printed PCL scaffolds

The MRI scan images of the beagle meniscus are reconstructed into a 3D model by Mimics software. Based on the 3D reconstruction of the meniscus model, the geometric design of the 3D printed meniscus scaffolds is carried out. According to the principle of discrete stacking, the micro-deposition 3D printing system prepares implantable degradable medical devices by layering superposition. The 3D meniscus model is discretized into different 2D sections according to a certain layer height, and the fiber filling path of each layer is planned.

To mimic the natural structure of the meniscus, the height of outer synovial margin (1.524 ± 0.023 mm) of the 3D printed bionic meniscus scaffolds is larger than that of inner free margin (0.482 ± 0.015 mm),

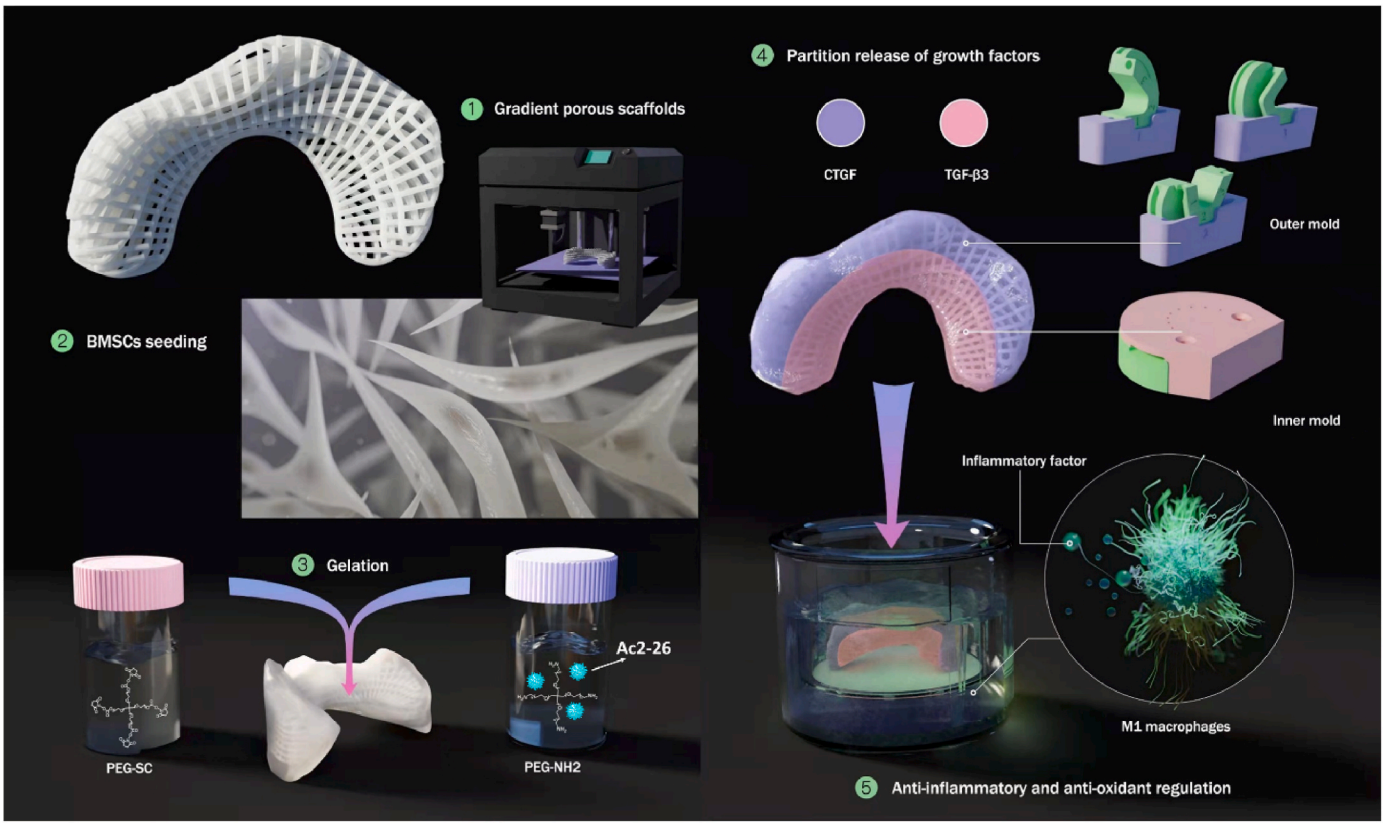

Fig. 1. Schematic illustration of the whole study. PCL meniscus scaffold was firstly fabricated with a gradient porous and heterogeneous structures. The third-passage BMSCs were seeded on the scaffolds. Then, we devised a rotation-immersion formulation in the metal mold to generate the PCL@tetra-PEG meniscus scaffold, in which tetra-PEG hydrogel not only improved biomechanical properties of PCL@tetra-PEG scaffold to match the native meniscus, but also provided opportunities on achieving variously regional encapsulation and spatiotemporal partition release of two human growth factors (CTGF and TGF-β3). Notably, the simultaneous encapsulation of Ac2-26 peptide within the composite scaffold could exert the anti-inflammatory and antioxidant effects on regulation of complex microenvironment to promote tissue regeneration.

which presents a gradient change of height. The outer radial screw spacing is 1.0 mm (L = 1.0 mm), and the gradual reduction is 0.6 mm (L = 0.6 mm) for the innermost radial screw spacing. The pitch of the screw in the circumferential direction on the same plane is uniform 0.6 mm (L = 0.6 mm). After completing the fiber deposition molding of one layer of cross-section, the system raises the nozzle height in the Z direction (h = 0.2 mm), carries out the order deposition of next layer of cross-section fibers, and then stacks the deposited fibers layer by layer to form a 3D bionic meniscus scaffolds support. By controlling the diameter, spacing and layer height of the deposited fibers, precise control of the pore structure inside the meniscus scaffolds can be achieved.

Different molecular weight PCL (40 kDa, 60 kDa and 80 kDa) particles are placed into the barrel. Set the barrel and nozzle heating temperature to 100 °C, and heat the particles to a molten state. The PCL fiber is evenly extruded from the nozzle with an inner diameter of 0.3 mm using a piston at a motion speed of 0.1 mm/min. The nozzle moves at a speed of 4 mm/s in the XY direction, depositing the fibers layer by layer on the working platform according to the pre-designed path. Finally, the preparation of PCL 3D multi-well meniscus scaffolds was achieved.

2.3. 3D printing mold design for the rotation-immersion formulation

MRI scan image was imported into the Mimics software to reconstruct the three-dimensional model of the meniscus, and imported into UG_NX design software to divide the meniscus into two areas, inside and outside, according to the shape of the meniscus. Two sets of molds were designed to shape the above two areas respectively, and then the molds are completed by 3D printing technology. The outer zone of rotation-immersion formulation was implemented with three immersion and rotation processes. The inner zone of rotation-immersion formulation was formed by one-time immersion.

2.4. Hydrogel preparation

Hydrogel was prepared by two components A and B. A was 4-arm poly(ethylene glycol)amine-20 K and B was 4-arm poly(ethylene glycol) succinimidyl ester-20 K. First, A and B were dissolved in sterile ddH2O with A solid content of 10%. Ac2-26 peptide was added to solution A. The final concentration of AC2-26 peptide was 80 μM. Two kinds of solution B were prepared and CTGF and TGF-β3 were added respectively. The final concentration of CTGF and TGF-β3 were 100 ng/mL and 10 ng/mL respectively. Mixing the solutions of A and B in a ratio of 1:1 could form a hydrogel, and a 3D printing mold was used to load different growth factors on the outer side (synovial edge, CTGF) and the inner side (free edge, TGF-β3) of meniscus scaffolds.

2.5. Release behavior of Ac2-26, CTGF and TGF-β3

The release kinetics of CTGF and TGF-β3 from tetra-PEG hydrogel were measured by incubating hydrogel (100 mg/mL) encapsulating CTGF into the phosphate-buffered saline (PBS) or TGF-β3 (0.1% bovine serum albumin) at 37 °C with mild agitation for up to 21 days. After centrifugation at 2500 rpm for 5 min, the supernatant of the hydrogel incubation solution was collected. Released CTGF and TGF-β3 concentration was measured using enzyme-linked immunosorbent assay (ELISA) kits following the manufacturer's protocols.

The released Ac2-26 peptide at different time points was isolated by filtration. Released peptide concentration was measured using Pierce

Quantitative Fluorometric Peptide Assay Kit following the manufacturer's protocols. The absorbance of these samples was measured at ex390/em475.

2.6. Anti-inflammatory and antioxidant activities examine of Ac2-26

Mouse macrophage RAW264.7 cells were pretreated with Ac2-26 for 4 h, and then LPS-induced ROS and RNS were detected by Cellular ROS/RNS Detection Assay Kit (Abcam, ab139473). Mouse macrophage RAW264.7 cells were stimulated with 100 ng mL^{-1} LPS for different times, and treated with Ac2-26 for the corresponding times at the same time. The intracellular iNOS, Arg-1 and COX2 expression levels in macrophages treated with LPS were analyzed by Western blot.

2.7. Bone marrow–derived MSC harvesting, culture, and seeding

Bone marrow–derived MSCs were isolated from 3-month-old New Zealand white rabbits. Isolation, culture, trilineage differentiation potential assay and immunophenotypic identification of MSCs were performed as previously described [39]. The cells seeded on the scaffolds were the third-passage MSCs.

Injection seeding was used to seed the MSCs to scaffolds. Cell suspension injection was performed by injecting the 80 μL of concentrated cell solution (1×10^5 cells) into the scaffold using a 25-gauge needle. Briefly, the cells were injected into the top/bottom/side face of the scaffold with a 25-gauge needle syringe. In order to study the cytotoxicity of hydrogel by live/dead assays, MSCs were firstly seeded into the PCL scaffold and the MSCs were filled with the entire scaffold. After immersing this PCL scaffold into the solution A containing the single cells suspension, the solution B with a ratio of 1:1 was further poured and mixed to form the PCL@tetra-PEG composite scaffold. In other words, the MSCs were spread throughout the PCL scaffold and tetra-PEG hydrogel.

2.8. Live/dead bacterial staining assay

The staining reagent mixture, a red fluorescent propidium iodide (PI) stain and a green fluorescent (AM) stain, was added to the reaction mixture and incubated in the dark at a room temperature for 15 min. The fluorescence emission of MSCs was assessed by means of confocal laser scanning microscopy (Olympus inverted confocal).

2.9. Biochemical stimulation

To investigate the effect of gradual pore meniscus scaffold cues on the differentiation of MSCs, uniform pore meniscus cellular scaffolds and gradual pore meniscus cellular scaffolds were treated as follows: CTGF (100 ng/mL, PeproTech), TGF-β3 (10 ng/mL, PeproTech), Fibrogenic induction supplement (ascorbic acid (50 μg/mL)) and chondrogenic induction supplement (0.1 μM dexamethasone, sodium pyruvate (100 μg/mL), L–ascorbic acid 2-phosphate (50 μg/mL), L-proline (40 μg/mL), and 1% 1 × insulin transferrin selenium (ITS)) for 3 weeks [8].

To explore the single or synergistic effect of spatiotemporal partition release of growth factors, anti-inflammatory and antioxidant regulation on the differentiation of MSCs, gradual pore meniscus cellular scaffolds were treated according to the following study groups: (i) the growth medium (-minimum essential medium (-MEM); Gibco BRL Co. Ltd.) as a control (no stimulus) and (ii) CTGF (100 ng/mL, PeproTech) and TGF-β3 (10 ng/mL, PeproTech) were non-temporally and non-spatially partitioned to induce differentiation of MSCs for 3 weeks. (iii) CTGF (100 ng/mL) and TGF-β3 (10 ng/mL) were temporally and spatially partitioned to induce differentiation of MSCs for 3 weeks (Spatiotemporal partition group). (iv) TEM and inflammatory cell models were co-cultured, CTGF and TGF-β3 were temporally and spatially partitioned to induce differentiation of MSCs for 3 weeks (Spatiotemporal partition/inflammation group). (v) TEM and inflammatory cell models were co-cultured, adjusted with Ac2-26 peptide, and CTGF and TGF-β3 were spatiotemporally partitioned to induce differentiation of MSCs for 3 weeks (Spatiotemporal partition/Inflammation/AC2-26 group). Fibrogenic induction supplement (ascorbic acid ((50 μg/mL)) and chondrogenic induction supplement (0.1 μM dexamethasone, sodium pyruvate (100 μg/mL), L–ascorbic acid 2-phosphate (50 μg/mL), L-proline (40 μg/mL), and 1% 1 × insulin transferrin selenium (ITS)) was included in the CTGF and TGF-β3 treatments, respectively [18].

2.10. Gene expression analysis

Total RNA was extracted using Trizol reagent (Invitrogen). Isolated RNA was reverse-transcribed and subjected to real-time PCR. The sequences of the primers for iNOS, Cox-2, TNF-α, Arg-1, IL-10, COL1A1, FN1, TNC, COL2A1, ACAN and SOX9 are shown in Table 1. The expression of GAPDH gene was evaluated as an internal control. The relative expression of the target gene was calculated by $^{\Delta\Delta}$CT method.

2.11. Immunofluorescence analyses

The scaffolds were washed by phosphate-buffered saline (PBS), fixed by 4% paraformaldehyde, blocked with 5% (v/v) bovine serum albumin in PBST at 37 °C for 60 min. The specimens were then incubated with primary antibodies against COL-1 (ab6308; Abcam; 1:300 dilution) and COL-2 (ab34712; Abcam; 1:300 dilution) at 4 °C for 24 h, followed by Alexa Fluor 488 Goat Anti-Rabbit IgG Antibody ReadyProbes Reagentor and 594 Goat Anti-Mouse IgG Antibody ReadyProbes Reagent (Invitrogen, USA) for 40 min at room temperature. The scaffolds were washed, stained with DAPI solution.

2.12. Western blot

The cells were washed twice with PBS and then lysed on ice in a 1 × lysis buffer (Cell Signaling) containing a mixture of proteases (Roche) and then subjected to sonication treatment. The proteins in cell lysates were separate by SDS-polyacrylamide gel electrophoresis gel (Fisher) according to their electrophoretic mobility. The proteins were then transferred to a membrane (PVDF), where they were stained with antibodies specific to the target protein (all from Abcam).

2.13. Mechanical analysis

As previously reported, the biomechanical properties of the scaffolds were evaluated using a material testing machine (AG-IS; Shimadzu). The elastic modulus was analyzed from the linear portion of the stress-strain curve. The 3D printed PCL gradual porous meniscus were compressed at a constant loading rate of 0.1 mm/min [8].

2.14. Statistical analysis

Parametric data were presented as the means ± standard deviation (SD). GraphPad Prism version 5.0 (California, USA) was used for the statistical analyses. All statistical comparisons between two groups were performed using the two-sided, nonpaired test. Differences were considered significant at $p < 0.05$.

3. Results

3.1. Anti-inflammatory and antioxidant properties of AC2-26 and phenotypic conversion of macrophages in vitro

In vitro inflammatory, oxidant regulation and M1 to M2 phenotypic changes of Raw264.7 cells were evaluated after incubation with Ac2-26. High concentrations of Ac2-26 peptide slightly inhibited the proliferation of MSCs but significantly promoted the proliferation of Raw264.7 (Fig. 2A and B). When the inflammation model was treated with low

Table 1
The primer sequences of genes.

Function	Gene	Forward primer(5′-3′)	Reverse primer(5′-3′)
M1 macrophage marker	iNOS	CCATCATGGACCACCACACA	CCATGCAGACAACCTTGGTG
	COX-2	GGGGTACCTTCCAGCTGTCAAAATCTC	GAAGATCTCGCCAGGTACTC ACCTGTATG
	TNF-α	TGTGCTCAGAGCTTTCAACAA	CTTGATGGTGGTGCATGAGA
M2 macrophage marker	Arg-1	ACAAGACAGGGCTCCTTTCAG	GGCTTATGGTTACCCTCCCG
	IL-10	CCAGTTTTACCTGGTAGAAGTGATG	TGTCTAGGTCCTGGAGTCCAGCAGACTCAA
Control (mouse)	GAPDH	GGTTGTCTCCTGCGACTTCA	TGGTCCAGGGTTTCTTACTCC
Fibrogenesis	COL1A1	CTCCCCAGATGTCTTACGGC	TCCGTCATCTCCGTTCTTGC
	FN1	CAAGCCTGGTTGTTACGACA	AGGTTCAGGTTTACTCTCGC
	TNC	TCTCTGCACATAGTGAAAAACAATACC	TCAAGGCAGTGGTGTCTGTGA
Chondrogenesis	COL2A1	TGCAGGAGGGGAAGAGGTAT	GGCAGTCCTTGGTGTCTTCA
	ACAN	GAGACCAAGTCCTCAAGCCC	CTCTGTCTCCTGGCAGGTTC
	SOX9	AGTACCCGCACCTGCACAAC	TACTTGTAGTCCGGGTGGTCTTTC
Control(rabbit)	GAPDH	GTATGATTCCACCCACGGCA	CCAGCATCACCCCACTTGAT

concentration of Ac2-26 peptide (10 μM), the ROS content was increased. With the increase of Ac2-26 peptide concentration, the ROS content gradually decreased, which was statistically significant (Fig. 2C). Similarly, the RNS content was also gradually decreased as the concentration of Ac2-26 peptide was increased (Fig. 2D). The experimental results proved that high concentrations of Ac2-26 peptide could effectively inhibit the overproduction of ROS and RNS in the total cells of macrophages stimulated by LPS for the first time.

Western blot was used to analyze the proinflammatory M1 markers, including inducible nitric oxide synthase (iNOS, involved in the overproduction of RNS (especially toxic NO)), cyclooxygenase-2 (Cox-2), and the expression of arginase 1 (Arg-1) (M2 anti-inflammatory macrophage marker protein). The protein expression of M1 biomarker iNOS and Cox-2 were significantly increased after LPS treatment. After incubation with Ac2-26 peptide, the expression of iNOS and Cox-2 significantly decreased compared to that of the untreated control as shown in Fig. 2E–G. When LPS-stimulated macrophages were treated with Ac2-26 peptide (80 μM) for 12 h, the expression of iNOS was significantly decreased (Fig. 2E).

The higher the concentration of AC2-26 peptide was, the more obviously iNOS protein expression was down-regulated (Fig. 2F), which further proved the inhibition effect of Ac2-26 peptide on the overproduction of RNS. After LPS-stimulated macrophages were treated with Ac2-26 peptide (80 μM) at different times, the expression of representative M2 marker Arg-1 was up-regulated (Fig. 2H). Similarly, Ac2-26 peptide treatment significantly down-regulated the mRNA expression levels of the proinflammatory M1 markers including iNOS, Cox-2 and TNF-α (Fig. 2I). In contrast, the anti-inflammatory M2 markers including Arg-1and IL-10 were markedly up-regulated after treatment with Ac2-26 peptide (Fig. 2I). The experimental results indicated that Ac2-26 peptide promoted the phenotypic conversion of M1 macrophages to M2 macrophages, which was beneficial to tissue remodeling.

3.2. Construction, biomechanics and biocompatibility of 3D-printed PCL gradual porous meniscus

The 3D reconstruction effect is highly consistent with the actual shape of the beagle meniscus, which meets the experimental needs and lays the foundation for further production of meniscus scaffolds (Fig. 3A). In this case, gradient porous meniscus scaffolds were printed using 3D printing technology. The free edge area (i.e., inner edge, Fig. 3B–b) had high fiber density and small pore size (average pore size was about 200 μm). While the edge of the synovial zone (i.e., the outer side, Fig. 3B–c) had a low fiber density and a large pore size (average pore size 400–500 μm). The two apertures each accounted for 1/2 width of the scaffold. Scanning electron microscope (SEM) showed that cells embedded on the surface and inside of the different molecular weight gradient porous meniscus scaffold (Fig. 3C and E). The mechanical behavior of PCL-4 group, PCL-6 group and PCL-8 group (the PCL meniscus scaffold with number-average molecular weight of 40 kDa, 60 kDa and 80 kDa) were similar to the natural meniscus in the compressive testing (Fig. 3D). It was mentioned that the hardness of PCL meniscus scaffolds was rigid and the toughness was relatively insufficient, which required to be improved for natural beagle meniscus. The biocompatibility of the PCL meniscus constructs with different molecular weight were evaluated by live/dead double staining *in vitro* and subcutaneous implantation *in vivo* (Figs. 3F and S1). Fig. 3F and Fig. S2 showed that PCL meniscus scaffold with a molecular weight of 60 kDa was better for the MSCs growth of than other groups.

3.3. Heterogeneity comparison of gradual and uniform pore meniscus scaffold

The heterogeneity of gradient porous TEM and uniform porous TEM was assessed by immunofluorescence and QPCR. We used PCL-6 meniscus scaffold as an example to verify the heterogeneous importance in Fig. 4. The seeded MSCs in gradual pore meniscus scaffold group with biochemical treatment showed zonal differentiation (inner versus outer) into a fibrochondrocyte-like cell phenotype with expression of both COL-1 and COL-2, which was similar to the native meniscus. In comparison, the uniform pore meniscus scaffold group could not exhibit zonal fibrochondrocyte differentiation of seeded MSCs (Fig. 4A).

The gradual pore meniscus scaffold group exhibited zonal variation (inner versus outer) in fibrogenic genes (COL1A1, FN1 and TNC) and chondrogenic genes (COL2A1, ACAN and SOX9), indicating the synergistic effects of gradual pore and biochemical treatment on the meniscus scaffolds (Fig. 4B). Furthermore, in the gradual pore meniscus scaffold group, the expression of fibrogenic genes (COL1A1, FN1 and TNC) was higher in the outer zones and the expression of chondrogenic genes (COL2A1, ACAN and SOX9) was higher in the inner zones, suggesting zone-specific mRNA phenotypes. The expression of fibrogenic genes (COL1A1 and TNC) was higher in the outer zones of gradual pore meniscus scaffold group and lower in the inner zones than those of uniform pore meniscus scaffold group. The expression of chondrogenic genes (COL2A1 and ACAN) was higher in the inner zones than those of uniform pore meniscus scaffold group while lower in the outer zones than those of uniform pore meniscus scaffold group. Collectively, the gradual pore meniscus scaffold was benefited to induce MSCs fibrochondrogenic differentiation and the specific zone expressions of COL-1 and COL-2 *in vitro*, which were more heterogeneous than those of uniform pore meniscus scaffold.

3.4. Construction, biomechanics and biocompatibility of different molecular weight of composite PCL@tetra-PEG meniscus scaffold

In order to enhance the biomechanics of PCL scaffold and improve surface hydrophilicity for meeting the requirement of native meniscus, the biocompatible tetra-PEG hydrogel was utilized to cover into the PCL scaffold to construct the composite PCL@tetra-PEG scaffolds using the rotation-immersion formulation in the metal mold (Fig. 5A). SEM

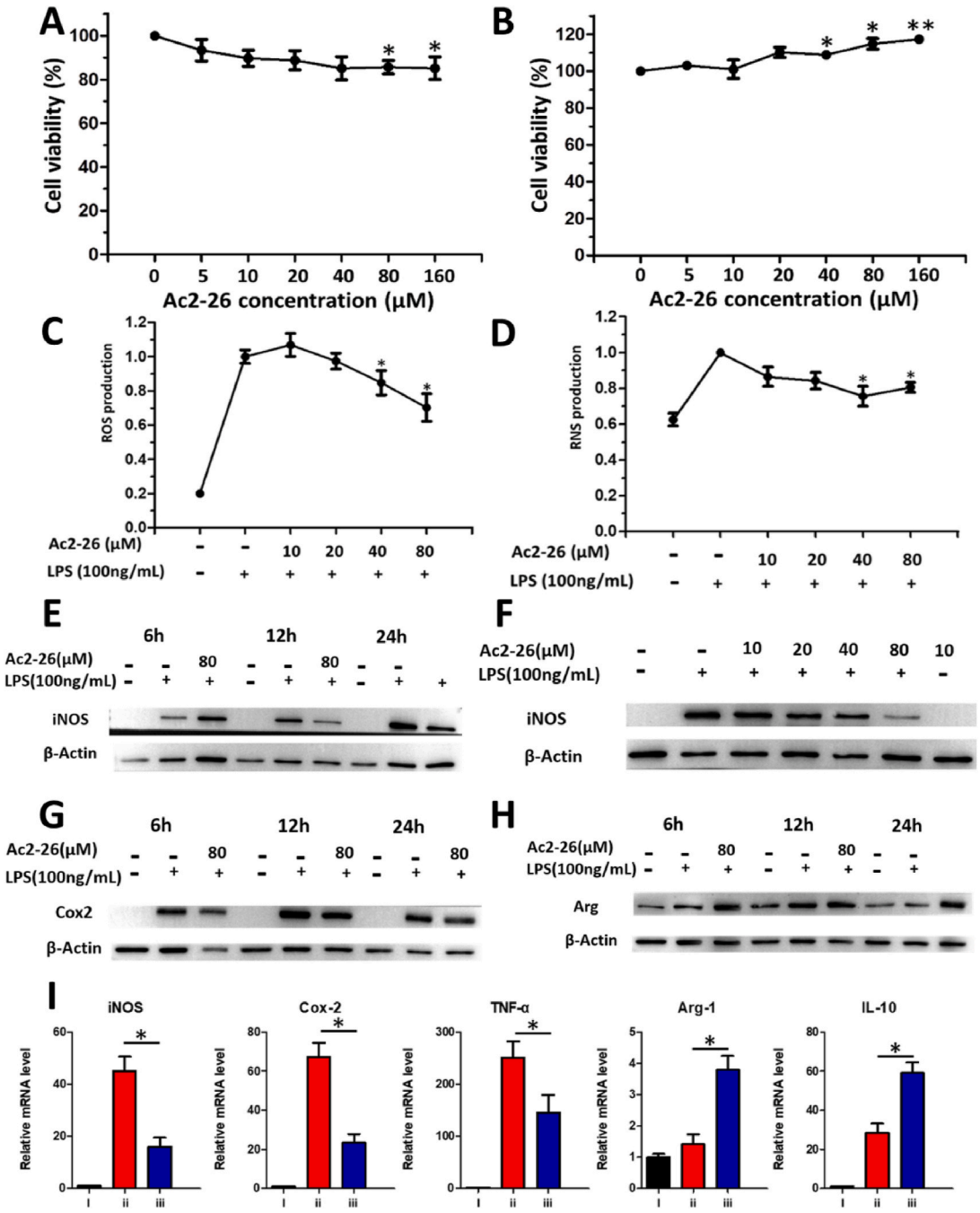

Fig. 2. Anti-inflammatory and antioxidant properties of AC2-26 and phenotypic conversion of macrophages *in vitro*. The viability of (A) MSCs and (B) Raw264.7 cells incubated at different concentrations of Ac2-26 mimetic Peptide of Annexin A1 for 24 h (n = 5). (C) ROS and (D) RNS content of Raw 264.7 stimulated by lipopolysaccharide (LPS) treated with different concentrations of Ac2-26. Western blot analysis of iNOS expression in LPS-stimulated macrophages treated with Ac2-26 for different times (E) and concentrations (F). Western blot analysis of intracellular COX2(G) and Arg-1 expression (H) in LPS-stimulated macrophages treated with Ac2-26 for different times. (I) mRNA expression of M1 and M2 macrophage markers in Raw 264.7 under various conditions by qRT-PCR analysis (n = 5). (i) Control group. (ii) LPS-stimulated group. (iii) LPS-stimulated macrophages treated with Ac2-26 for 12 h. Differences were considered significant at $^{*}p < 0.05$.

images showed that the hydrogels could be embedded on the surface and inside of the different molecular weight gradient porous meniscus scaffold (Fig. 5B). Importantly, these composite PCL@tetra-PEG meniscus constructs with different molecular weight displayed the excellent biocompatibility and improved mechanical performance. The live/dead double staining results revealed that favorable safety of tetra-PEG hydrogel on the growth of the MSCs (Figs. 5C and S2). Both PCL-4@tetra-PEG and PCL-6@tetra-PEG groups exhibited few dead cells, and there was no significant difference in the proportion of dead cells, revealing the favorable safety of scaffolds on the growth of the MSCs. After 3D-printed PCL scaffolds were composited with tetra-PEG hydrogel, the compressive strength range of scaffold became larger and the toughness of scaffolds was obviously improved. Notably, the PCL@tetra-PEG meniscus scaffold with a molecular weight of 60 kDa was nearly equal to the true value of native beagle meniscus (Fig. 5D). The degradation behavior of the PCL@tetra-PEG scaffold with different molecular weight in PBS (pH 7.4) was similar over time (Fig. S3).

In addition to the improvement of the hardness and the toughness, the introduction of tetra-PEG hydrogel also provided the opportunities on achieving variously regional encapsulation and spatiotemporal

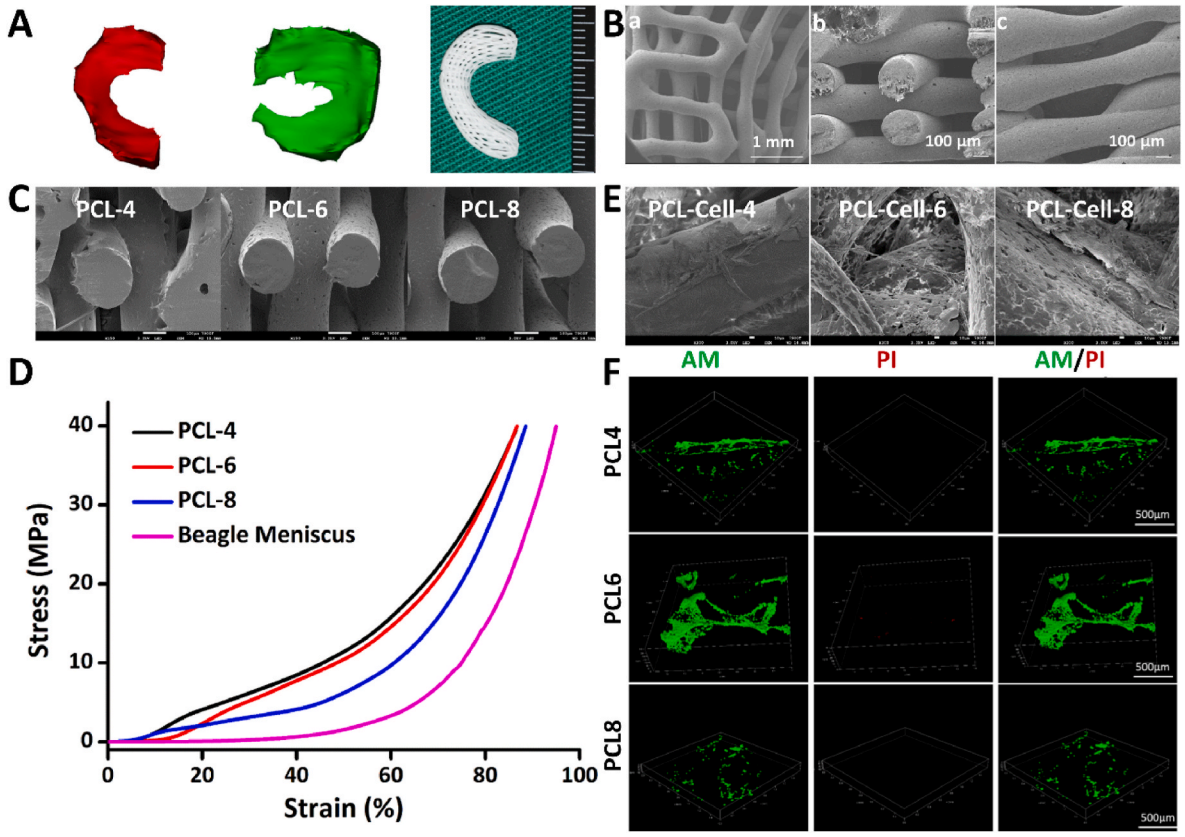

Fig. 3. Construction, biomechanics and biocompatibility of 3D-printed PCL gradual porous meniscus. (A) Mimics 3D reconstruction and 3D printing gradual porous beagle meniscus. (B) SEM of gradient porous meniscus scaffold. (a) The whole frame; (b) the free zone, had high fiber density and small pore size (average pore size was about 200 μm); (c) the synovial zone, had a low fiber density and a large pore size (average pore size 400–500 μm). (C) SEM of gradient porous meniscus scaffolds with different number-average molecular weight. Scale bar:100 μm. (D) Mechanical behaviors of different PCL scaffolds and beagle meniscus. (E) SEM images of different molecular weight gradient porous meniscus scaffolds with seeded MSCs. Scale bar:10 μm. (F) Live/Dead Double Staining of MSCs in PCL scaffolds with different molecular weights.

partition release of two human growth factors. Using the rotation-immersion formulation in the metal mold, composite PCL@tetra-PEG meniscus scaffolds were constructed with simultaneous capsulation of CTGF and TGF-β3 growth factors in synovial zone and free edge zone, respectively (Fig. 5A). CTGF and TGF-β3 factors could induce endogenous stem/progenitor cells to differentiate and synthesize zone-specific type I and II collagens. On account of the size difference, the CTGF factor was firstly released and then followed by TGF-β3. The relatively rapid release of CTGF from the outer layer and the slower release of TGF-β3 from the inner layer lasted for 21 days in their respective areas (Fig. 5E). Notably, the functional Ac2-26 peptide was also simultaneously encapsulated and dispersed into the whole composite PCL@tetra-PEG meniscus scaffold, which could sustain over one week (Fig. 5F), indicating the negligible effects on these two factors. For the *in vitro* construct, the PCL-6@tetra-PEG group had the best values with increased aggregate modulus and matched ductility compared to the natural beagle meniscus. All the results clearly demonstrated that the PCL@tetra-PEG meniscus scaffold possessed favorable biomechanical properties and biocompatibility like the natural beagle meniscus.

3.5. Spatiotemporal partition releasing dual growth factors and anti-inflammatory and antioxidant regulation on fibrochondrocyte differentiation of MSCs

To reconstruct meniscus tissues with natural morphology and heterogeneity, signaling biomolecules and biomechanical stimuli are required in the cellular microenvironment. As typical representatives of biomechanical stimulation, TGF-β3 growth factor can show the up-regulation of fibro-chondrogenesis and chondrogenic gene expression (COL2A1, ACAN and SOX9) [32,33]. While the CTGF growth factor can up-regulate the expression of fibro-chondrogenesis and fibrogenesis genes (COL1A1, FN1 and TNC) through appropriate biomechanical stimulation [8,34,35].

Regional release of growth factors and anti-inflammatory and anti-oxidant regulation synergistically induce fibrochondrocyte differentiation of MSCs. After filling the scaffold with seeded MSCs, CTGF and TGF-β3 factors were non-spatiotemporally partitioned (non-spatiotemporal partition group) or spatiotemporally partitioned (spatiotemporal partition group) to induce differentiation of MSCs for 3 weeks. At same time, TEM and inflammatory cell models were co-cultured (spatiotemporal partition/inflammation group) and treated with Ac2-26 peptide (spatiotemporal partition/inflammation/AC2-26 group). The outer and inner layers of native meniscus tissue specifically expressed type I and type II collagens.

The seeded MSCs in PCL meniscus scaffold with a molecular weight of 60 kDa showed higher expression of COL-1 in the outer layer and expression of COL-2 in the inner layer than those in the PCL meniscus scaffold with a molecular weight of 40 kDa. The expression of COL-1 in the outer layer and expresstion of COL-2 in the inner layer were higher in PCL meniscus scaffold with a molecular weight of 40 kDa than those in PCL meniscus scaffold with a molecular weight of 80 kDa (Fig. 6,S4-7). The fibrogenic genes (COL1A1, FN1 and TNC) and chondrogenic genes (COL2A1, ACAN, and SOX9) in MSCs in the inner and outer regions of 60 kDa gradient porous meniscus scaffold group were highly expressed than 40 kDa gradient porous meniscus scaffold group (Fig. 7). The expression of fibrogenic genes (COL1A1, FN1 and TNC) and

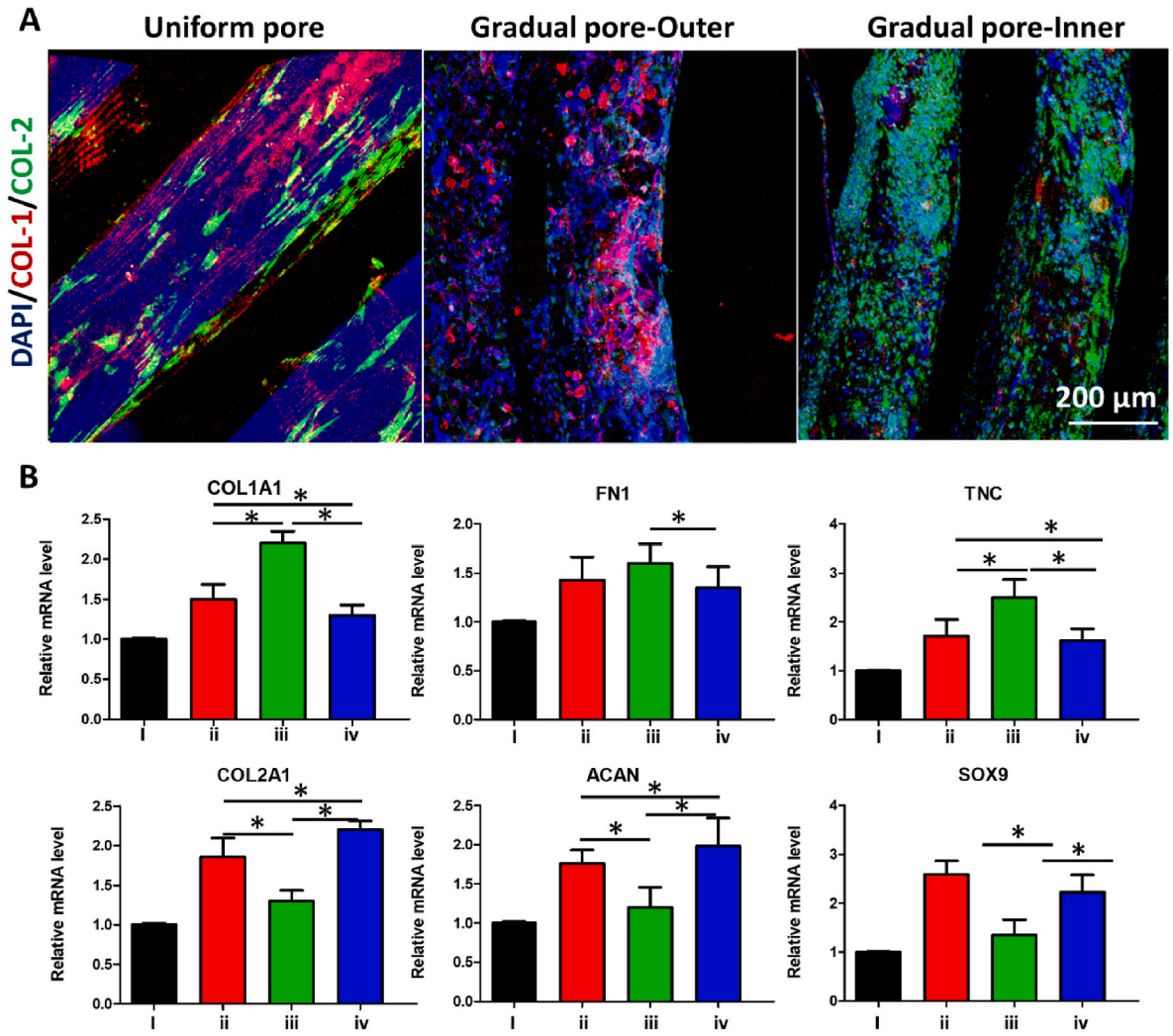

Fig. 4. Heterogeneity comparison of gradual and uniform pore meniscus scaffold. (A) Immunofluorescence of the expression of COL-1 (collagen I, red) and COL-2 (collagen II, green) in uniform and gradual pore meniscus scaffold. (B) Analysis of the gene expression of chondrocyte phenotypes in uniform and gradual pore meniscus scaffold. (i) Growth medium is used as a control (No stimulus group). (ii) MSCs seeded on the uniform pore meniscus scaffolds were differentiated with CTGF and TGF-β3 for 3 weeks (Uniform pore group). (iii) MSCs seeded on the outer regions of gradual pore meniscus scaffolds were differentiated with CTGF and TGF-β3 for 3 weeks (Gradual pore-outer group). (iv) MSCs seeded on the inner regions of gradual pore meniscus scaffolds were differentiated with CTGF and TGF-β3 for 3 weeks (Gradual pore-inner group). Differences were considered significant at $^{*}p < 0.05$.

chondrogenic genes (COL2A1, ACAN and SOX9) in MSCs in the inner and outer regions of 8 kDa gradient porous meniscus scaffold group were lower than those in 40 kDa gradient porous meniscus scaffold group (Fig. 7). The results indicated that PCL meniscus scaffold with a molecular weight of 60 kDa was best for the construction of heterogeneous meniscus.

The seeded MSCs showed zonal differentiation into a fibrochondrocyte-like cell phenotype with COL-1 expressed in the outer layer and Col-2 expressed in the inner layer in the group with spatiotemporal partition treatments or non-spatiotemporal partition treatments, which was similar to the natural meniscus (Figs. 6, 7, and S4-7). Furthermore, fibrosis genes (COL1A1, FN1 and TNC) were highly expressed in the outer layer, while chondrogenic genes (COL2A1, ACAN and SOX9) were highly expressed in the inner layer in both groups, suggesting the zone-specific mRNA phenotypes. It was attributed to that the gradient porous scaffold itself was conducive to the formation of heterogeneous meniscus. However, the expression of fibrogenic genes (COL1A1, FN1 and TNC) and chondrogenic genes (COL2A1, ACAN and SOX9) in MSCs in the inner and outer regions of non-spatiotemporal partition group were lower than those in spatiotemporal partition group (Fig. 7), further revealing the significant roles of spatiotemporal partition release on promoting the formation of heterogeneous meniscus on the basis of gradient porous scaffold.

The TEM and inflammatory cell models were co-cultured in the spatiotemporal partition/inflammation group. The concentrations of various mediators in culture medium from no stimulus group (i), spatiotemporal partition/inflammation group (ii) and spatiotemporal partition/inflammation/AC2-26 group (iii) were measured by Luminex detection technology (Fig. S8). There was no zonal fibrochondrocyte differentiation of MSCs in the scaffold, suggesting that inflammation could effectively inhibit the zone-specific differentiation and expression of chondrocyte phenotypes COL-1 and COL-2 in TEM. The spatiotemporal partition/inflammation groups were treated with Ac2-26 in the spatiotemporal partition/inflammation/AC2-26 group. Zone-specific protein expression and mRNA phenotypes in spatiotemporal partition/inflammation/AC2-26 group were similar to the spatiotemporal partition group and natural meniscus (Figs. 6, 7 and S4-7), which indicated that AC2-26 peptides could improve the zone-specific differentiation and expression of chondrocyte phenotypes under inflammatory stimulation.

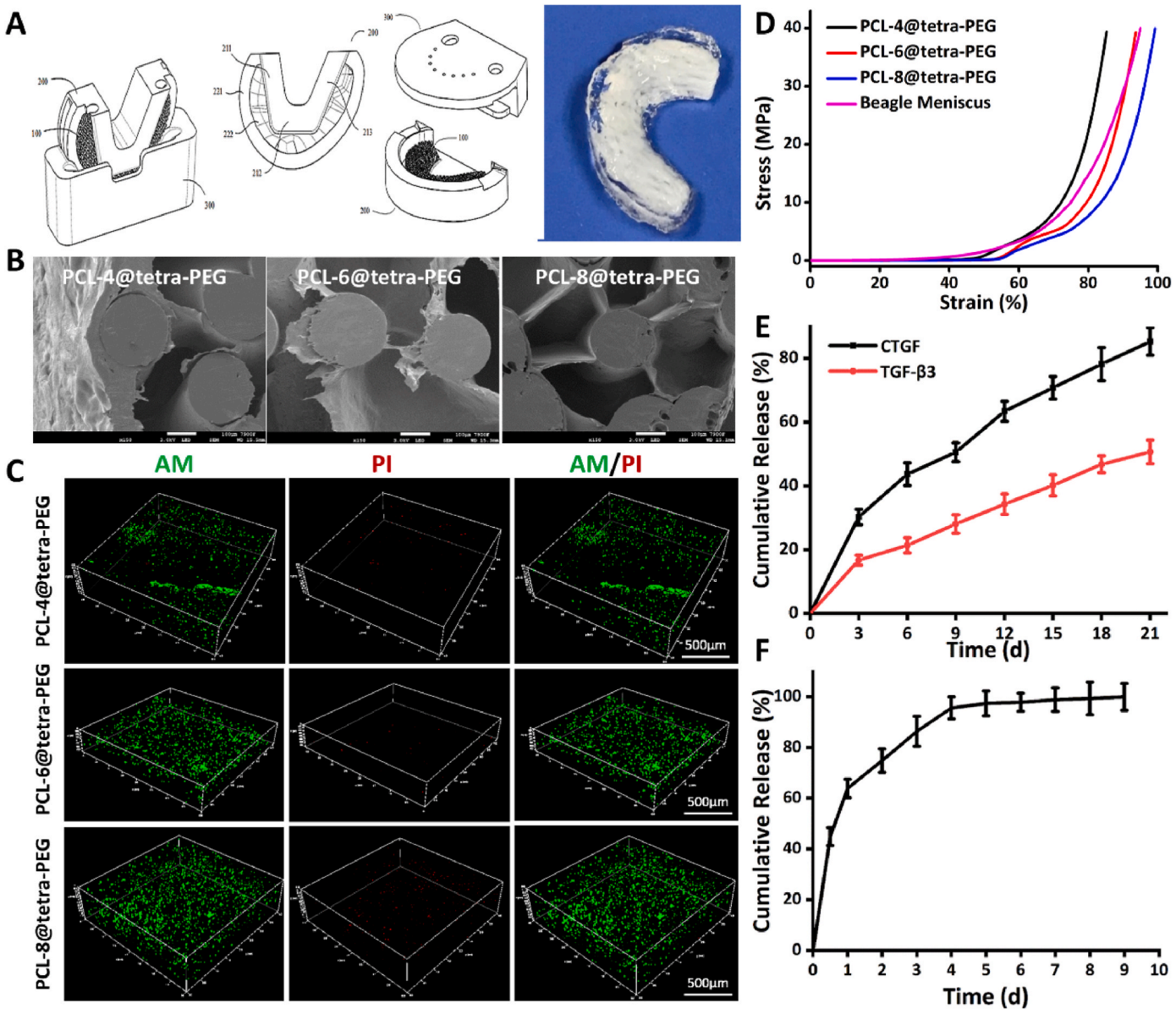

Fig. 5. Construction, biomechanics and biocompatibility of different molecular weight of composite PCL@tetra-PEG meniscus scaffold. (A) Rotation-immersion formulation for partition release of CTGF and TGF-β3 growth factors by 3D printing mold. (B) SEM images and (C) Live/dead double staining of MSCs in composite PCL@tetra-PEG meniscus scaffolds with different molecular weights. (D) Mechanical behaviors of composite PCL@tetra-PEG meniscus scaffolds with different molecular weights. *In vitro* cumulative release curve of (E) CTGF and TGF-β3 and (F) Ac2-26 peptide incubated at 37 °C (mean ± SD, n = 5). The released peptide at different time was isolated by filtration, and the absorbance of these samples was measured at ex390/em475.

4. Discussion

We extend the research on the basis of our previous research without using a customized dynamic tension-compression loading system in conjunction with two growth factors [8]. The purpose of this study was to explore the synergistic effect of gradient porous scaffolds design, spatiotemporal partition release of growth factors and anti-inflammatory and antioxidant regulation in inducing the differentiation of MSCs seeded onto composite PCL@tetra-PEG scaffolds and reconstruction of tissue-engineered meniscus. The biomechanical and biological properties of the constructs were evaluated *in vitro*. Anti-inflammatory and anti-oxidant treatments had been shown to successfully regenerate meniscus fibrochondral tissue under inflammatory and oxidative microenvironmental conditions, and the anisotropic properties were comparable to those of natural meniscus. The results highlighted the potency of orchestrated structural, anti-inflammatory and antioxidant, and biochemical stimuli for engineering of regenerated anisotropic tissue.

The physiological anisotropy could be induced using a customized dynamic tension-compression loading system in conjunction with two growth factors in the TEM. However, TEM was susceptible to contamination during compression-tension strains process. 3D printing of biological tissues had been of increasing interest to the biomaterial community in part because of its potential to produce spatially heterogeneous constructs [15]. Systematic investigations of gradients in biological materials were challenging because variations in material architecture or loading conditions were accompanied by the differences in mechanical design. Recently, advancements in the manufacturing of complex soft and stretchable gradients had been demonstrated using new material formulations or processing strategies. Stephanie Rhee et al. focused on developing and evaluating a 3D bioprinting technique of spatially heterogeneous collagen constructs for cartilage tissue

engineering [36–38]. Whether 3D printing gradient porous scaffolds could replace the biomechanical stimulation to construct a heterogeneous TEM remains to be explored. With the help of 3D printing technology, we printed gradient porous meniscus scaffolds using biodegradable PCL materials (Fig. 3B–a). Immunofluorescence and genes expression results showed that the inner and outer regions of gradient porous TEM could express COL1A1 and COL2A1, which were more heterogeneous than uniform porous TEM (Fig. 4). Collectively, the gradual pore meniscus scaffold was beneficial to induce MSCs fibrochondrogenic differentiation and the specific zone expressions of COL1A1 and COL2A1 *in vitro*. The reason for the formation of heterogeneity was due to that the edge of the synovial zone had a low fiber density and a large pore size, and the free edge area had high fiber density and small pore size. The large pore size (average pore size of 400–500 μm) promoted the expression of fibrosis genes (COL1A1, FN1 and TNC). The small pore size (average pore size of 200 μm) was conducive to the expression of chondrogenic genes (COL2A1, ACAN and SOX9).

PCL is extensively employed in various areas of biology and medicine, particularly in tissue engineering applications. The intrinsic PCL properties of molecular weight, surface roughness, modulus and mechanics play a significant role in stem cell fate and tissue regeneration. Many studies discuss the various types of scaffolding approaches including cellular and acellular approach used in the field of tissue engineering and more importantly their future prospects in tissue regeneration efforts. However, there is no relevant research studying the effect of meniscus scaffolds with different molecular weights on the construction of tissue engineering meniscus (TEM). In this work, we explored the optimal molecular weight of PCL scaffolds for the construction of heterogenous TEM. Our results showed that although the mechanical property of PCL-8 group exhibited higher than PCL-4 and PCL-6 groups in the compressive conditions (Fig. 3D), the biocompatibility of PCL-8 group was obviously poor compared to the other groups (Fig. 3F). Therefore, PCL-6 was selected as a most suitable scaffold for building heterogeneous TEM. In addition, the printing process with the circumferential and radial orientation may also cause the difference of microstructure, heterogeneity and biomechanical properties of PCL meniscus scaffold. From this part of the results, we can conclude that 3D printing gradient porous scaffolding can be used to replace biomechanical stimuli to heterogeneous TEM. However, its biomechanical properties need to be further improved to match the native meniscus.

Our study also explores whether the spatiotemporal partition release of two growth factors using a novel rotation-immersion formulation method could enhance the effect of heterogeneous structure induced by 3D printing gradient porous scaffolding. The common characteristic of many biological tissues and organs was inhomogeneity [39–41]. Meniscus regeneration required not only the restoration of structural heterogeneity, but also the ability to perform functional heterogeneity at the cellular and stromal level similar to the regeneration of the lungs, heart and blood vessels. Studies have shown that meniscus regeneration with heterogeneous tissue properties and function could be achieved through protein-releasing cellular biomaterial scaffolds. Current strategies upon spatiotemporal release of CTGF and TGF-β3 offered ready-to-use grafts for tissue engineering [18]. To perform mechanical and biochemical functions similar to the regeneration of meniscus, the 3D-printed meniscus scaffolds were composited with biocompatible tetra-PEG hydrogel in situ. In this work, we used a novel rotation-immersion formulation method to prepare the composite PCL@tetra-PEG meniscus scaffold, which not only improved the mechanical functions of pure PCL scaffold but also acquired advanced chances to achieve the variously regional encapsulation and spatiotemporal partition release of two human growth factors, exhibiting the multiple tissue phenotypes with heterogeneous functions. In fact, the amine groups distributed in the cytokines and peptide can also react with the active ester of residual tetra-PEG-SC polymer within the tetra-PEG hydrogels. Therefore, a portion of CTGF and TGF-β3 can be bonded into the tetra-PEG-SC aqueous solution (B). Moreover, although the Ac2-26 had a weak electrostatic interaction with tetra-PEG-NH_2 aqueous solution (A), the solutions A and B were quickly mixed together, thus also generating the chemical bonding within seconds in the hydrogels. In this case, the cytokines and peptide can achieve the slowly sustained release. However, on account of the dimensional variation, these cytokines and peptide displayed various release rate from the tetra-PEG hydrogels.

After composition with soft tetra-PEG hydrogel, the range of compressive strength becomes larger for the PCL@tetra-PEG meniscus scaffold, wherein the PCL-6@tetra-PEG group exhibited the best values with suitable biocompatibility and matched biomechanical properties compared to the natural beagle meniscus (Fig. 5). In addition, the release of CTGF and TGF-β3 in various areas *in vitro* led to the respective formation of fibrochondral phenotypes, which could induce the specific differentiation of MSCs to express type I and type II collagen (Figs. 6 and 7). CTGF and TGF-β3 could induce repeated derivation of fibrochondrocytes from postnatal MSC, which may have broad implications for the regeneration of other fibrochondrocytes.

Furthermore, our research also studied whether anti-inflammatory and anti-oxidant microenvironment could improve the construction quality of TEM. Resolution of inflammation involved a delicate balance between pro-inflammatory and anti-inflammatory, which was a highly complex process [42,43]. Failed resolution of inflammation was a potential component of several common diseases, so there were considerable interests in developing treatments that enhanced this effect [44]. As an active N-terminal peptide of an endogenous proresolving protein annexin A1, Ac2-26 peptide was promising for the management of tissue engineering meniscus due to its multiple anti-inflammatory effects [45,46]. Ac2-26 showed tissue protection in animal models of inflammation, such as peritonitis and atherosclerosis [29]. A recent study revealed the potential of Ac2-26 to treat colitis by injecting Ac2-26 nanoparticles into the peritoneum or mucosa [30]. Compared with traditional therapies such as mesolamine, aspirin and dexamethasone, Ac2-26 therapy had the ability to imitate or induce the natural resolution of inflammation without any side effects [31]. The latest study found that a smart nanotherapy (i.e., oxidation-reactive nanoparticles containing Annexin A1-mimetic peptide Ac2-26) can respond to the highly expressed ROS in the diseased site and release the loaded Ac2-26 reactively [47]. Ac2-26 polymer nanoparticles can reduce the level of chronic inflammation in mouse models of atherosclerosis [30], and also improve the healing in mouse models of colitis or colonic wounds [31].

In the present study, we investigated the encapsulation, delivery and biological function of the Ac2-26 peptide. We examined the mechanisms underlying the therapeutic effects of Ac2-26 *in vitro*. High concentrations of Ac2-26 peptide slightly inhibited the proliferation of BMSCs (Fig. 2A). However, high concentration of Ac2-26 peptide promoted the proliferation of Raw264.7 cells, which was significantly different (Fig. 2B). Ac2-26 effectively reduced ROS generation and RNS generation and inflammatory response in stimulated macrophages. The mechanism of intracellular ROS and RNS reduction may be that Ac2-26 could reduce the oxidative stress-induced apoptosis by eliminating intracellular ROS. Ac2-26 could further effectively inhibit macrophages apoptosis and reduce ROS production and inflammation in stimulated macrophages. Moreover, Ac2-26 effectively switched macrophages from a proinflammatory M1 phenotype toward an anti-inflammatory M2 phenotype, further reducing the production of proinflammatory cytokines and increasing the release of proresolving molecules (Fig. 2), which were consistent with previous literatures [47–50]. According to above analysis, it was speculated that Ac2-26 could effectively reduce the expression of pro-inflammatory mediators, weaken the transport and infiltration of inflammatory cells, promote the endocytosis of apoptotic neutrophils, and increase the phenotypic transition of macrophages.

Fahy. et al. found that MSC chondrogenesis was inhibited by factors secreted by synovial macrophages and M1 macrophages were potential mediators of the anti-chondrogenic effect [51]. In addition to

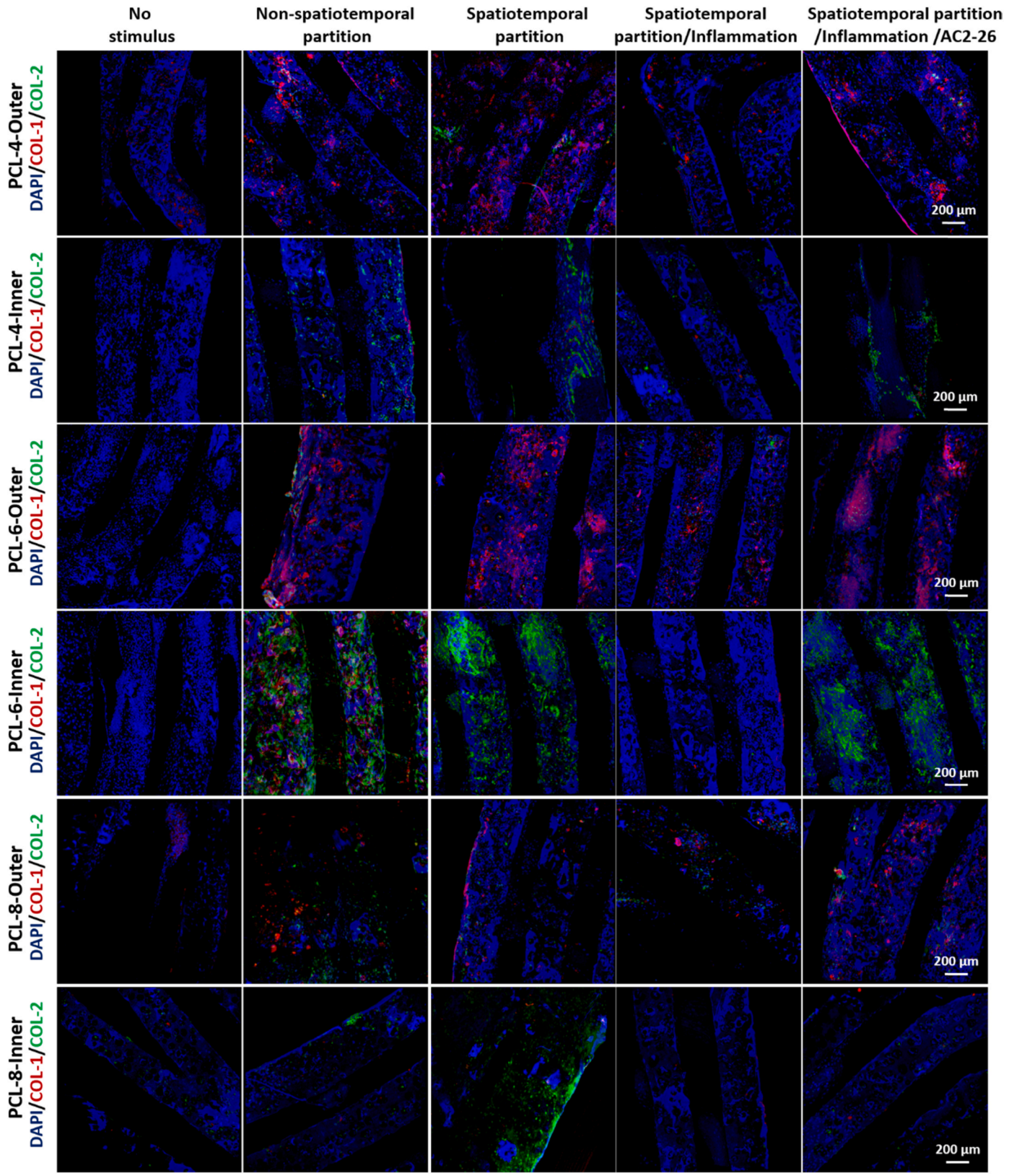

Fig. 6. Regional release of growth factors and anti-inflammatory and antioxidant regulation synergistically induce fibrochondrocyte differentiation of MSCs. Immunofluorescence to observe the expression of COL-1 (collagen I, red) and COL-2 (collagen II, green). (i) The growth medium is used as a control (No stimulus group). (ii) CTGF and TGF-β3 were non-temporally and non-spatially partitioned to induce differentiation of MSCs for 3 weeks (non-spatiotemporal partition group). (iii) CTGF and TGF-β3 were temporally and spatially partitioned to induce differentiation of MSCs for 3 weeks (Spatiotemporal partition group). (iv) TEM and inflammatory cell models were co-cultured and CTGF and TGF-β3 factors were temporally and spatially partitioned to induce differentiation of MSCs for 3 weeks (spatiotemporal partition/inflammation group). (v) TEM and inflammatory cell models were co-cultured after treatment with Ac2-26 peptide, and CTGF and TGF-β3 were spatiotemporally partitioned to induce differentiation of MSCs for 3 weeks (spatiotemporal partition/inflammation/AC2-26 group).

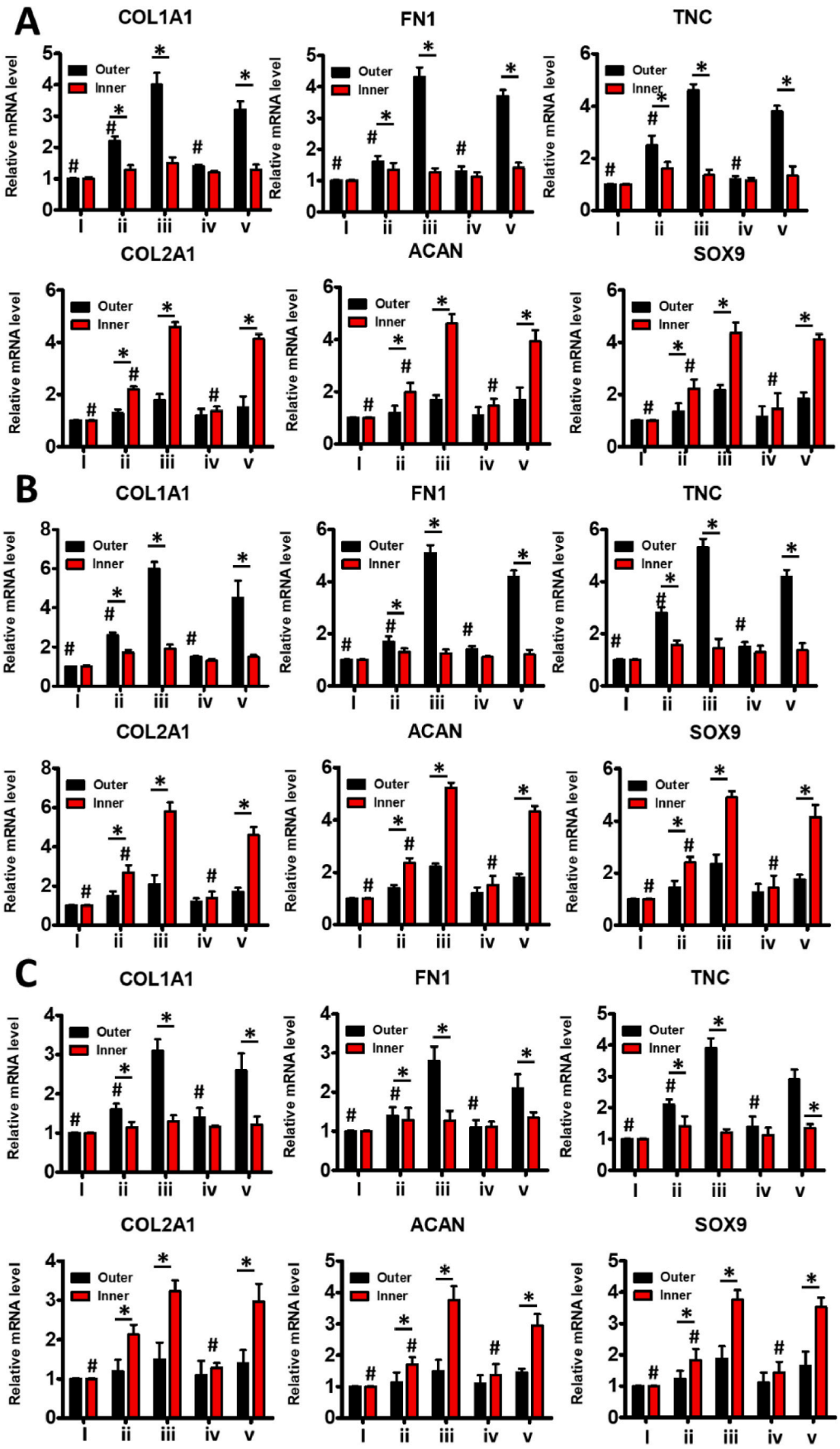

Fig. 7. Analysis of the gene expression of growth factor partition release and anti-inflammatory and antioxidant regulation synergistically inducing fibrochondrocyte differentiation of MSCs. (A–C) Expression of fibrogenic genes (COL1A1, FN1, and TNC) and chondrogenic genes (COL2A1, ACAN, and SOX9) in MSCs in the inner and outer regions of 40 kDa, 60 kDa and 80 kDa gradient porous meniscus scaffold. (i) The growth medium is used as a control (No stimulus group). (ii) CTGF and TGF-β3 were non-temporally and non-spatially partitioned to induce differentiation of MSCs for 3 weeks (non-spatiotemporal partition group). (iii) CTGF and TGF-β3 were temporally and spatially partitioned to induce differentiation of MSCs for 3 weeks (Spatiotemporal partition group). (iv) TEM and inflammatory cell models were co-cultured and CTGF and TGF-β3 factors were temporally and spatially partitioned to induce differentiation of MSCs for 3 weeks (spatiotemporal partition/inflammation group). (v) TEM and inflammatory cell models were co-cultured after treatment with Ac2-26 peptide, and CTGF and TGF-β3 were spatiotemporally partitioned to induce differentiation of MSCs for 3 weeks (spatiotemporal partition/inflammation/AC2-26 group). $*P < 0.05$ between the inner region and outer region in the same group; $\#P < 0.05$ between the spatiotemporal partition group and other groups in the same region (outer zone for fibrogenic genes; inner zone for chondrogenic genes). All data are presented as means ± SD (n = 6) and and were analyzed by two-sided, nonpaired test.

controlling the regional release of CTGF and TGF-β3, our results demonstrated that Ac2-26 peptide could also be simultaneously encapsulated into tetra-PEG hydrogel with controlled temporal release behavior (Fig. 5F). Inflammation could inhibit the zone-specific differentiation and expression of chondrocyte phenotypes COL-1 and COL-2 in TEM (Figs. 6 and 7). However, the anti-inflammatory and antioxidant regulation of AC2-26 peptides improved the zone-specific differentiation and expression of chondrocyte phenotypes under inflammatory stimulation, which highlighted the potency of the anti-inflammatory and antioxidant regulation of AC2-26 peptides for the regenerated meniscus. In this study, we explored the synergistic effects of 3D printing technology, spatiotemporal partition release manipulation and anti-inflammatory and antioxidant regulation in inducing the differentiation of MSCs seeded onto biomaterial scaffolds and reconstruction of tissue-engineered meniscus, which could provide a theoretical basis for cultivating clinically valuable TEM. Although synergistic effects could lead to a fibrochondrogenic phenotype, the *in vivo* actions of released growth factors and peptides should be best judged by the quality of the consistent yield of fibrocartilage *in vivo* in the further research.

5. Conclusion

In summary, we prepared a novel biomimetic PCL@tetra-PEG meniscus scaffold by 3D printing technology and rotation-immersion formulation in the 3D-printed metal mold, which could replace the biomechanical stimulation to construct a regional and functional heterogeneous TEM. By integrating the synergistic advantages of 3D-printing gradient porous meniscus, spatiotemporal partition release of two growth factors and anti-inflammatory and antioxidant regulation, this composite PCL@tetra-PEG meniscus scaffold possessed biomimetic morphology, mechanics, heterogeneity and functionality to native meniscus. Remarkably, the release of Ac2-26 peptide from the meniscus scaffold could effectively suppress inflammation, facilitated the convert of macrophages phenotype from a pro-inflammatory M1 macrophages to an anti-inflammatory M2 macrophages, improve the zone-specific differentiation and expression of chondrocyte phenotypes under inflammatory stimulation. Therefore, this synergistic strategy evidently improved the smart construction level of tissue engineered bionic meniscus scaffolds, and we believe this strategy can also be efficiently extended to other tissue engineering applications.

Ethics approval and consent to participate

This study was approved by the Ethics Committee of Peking University Third Hospital (protocol reference #A2020128).

CRediT authorship contribution statement

Bingbing Xu: Conceptualization, Investigation, Methodology, Project administration, Writing – original draft. **Jing Ye:** Data curation, Formal analysis, Investigation, Writing – review & editing, Project administration, Funding acquisition, Supervision, Writing – review & editing. **Bao-Shi Fan:** Methodology, Investigation, Resources, Writing – review & editing. **Xinjie Wang:** Data curation, Methodology. **Ji-Ying Zhang:** Data curation, Investigation. **Shitang Song:** Data curation, Investigation. **Yifan Song:** Data curation, Methodology. **Wen-Bo Jiang:** Resources, Methodology. **Xing Wang:** Writing – review & editing.

Declaration of competing interest

The authors declare that they have no known competing financial interests or personal relationships that could have appeared to influence the work reported in this paper.

Acknowledgments

This research was funded by the National Natural Science Foundation of China (NSFC, 82002298, 51920105006, 51973226), the China Postdoctoral Science Foundation (2020M670066), the National Key Research and Development Program of China (2016YFC1100704), and the Youth Innovation Promotion Association CAS (2019031). We would like to thank Teacher Xiaoyan Cao for her guidance and help in the compression experiments.

Appendix A. Supplementary data

Supplementary data to this article can be found online at https://doi.org/10.1016/j.bioactmat.2022.05.019.

References

[1] E.A. Makris, P. Hadidi, K.A. Athanasiou, The knee meniscus: structure-function, pathophysiology, current repair techniques, and prospects for regeneration, Biomaterials 32 (30) (2011) 7411–7431.
[2] P. Helder, F.C. Ibrahim, S.C. Joana, et al., Histology-ultrastructure-biology, Surg. Meniscus (2016) 23–33.
[3] K. Pihl, M. Englund, L.S. Lohmander, et al., Signs of knee osteoarthritis common in 620 patients undergoing arthroscopic surgery for meniscal tear, Acta Orthop. 88 (1) (2016) 1–6.
[4] I.F. Cengiz, H. Pereira, J. Espregueira-Mendes, et al., Treatments of meniscus lesions of the knee: current concepts and future perspectives, Regen. Eng. Translat. Med. 3 (1) (2017) 32–50.
[5] Z.Z. Zhang, S.J. Wang, J.Y. Zhang, et al., 3D-printed poly(ε-caprolactone) scaffold augmented with mesenchymal stem cells for total meniscal substitution, Am. J. Sports Med. 45 (7) (2017) 1497–1511.
[6] P.A. Mouthuy, S.J.B. Snelling, S.G. Dakin, et al., Biocompatibility of implantable materials: an oxidative stress viewpoint, Biomaterials 109 (2016) 55–68.
[7] C. Ma, M.L. Kuzma, X. Bai, et al., Biomaterial-based metabolic regulation in regenerative engineering, Adv. Sci. 6 (2019) 1900819.
[8] Z.Z. Zhang, Y.R. Chen, S.J. Wang, et al., Orchestrated biomechanical, structural, and biochemical stimuli for engineering anisotropic meniscus, Sci. Transl. Med. 11 (487) (2019), eaao0750.
[9] K.A. Athanasiou, J. Sanchez-Adams, Engineering the knee meniscus, Synth. Lect. Tissue Eng. 1 (1) (2011) 1–97.
[10] Herman S. Cheung, Distribution of type I, II, III and V in the pepsin solubilized collagens in bovine menisci, Connect. Tissue Res. 16 (4) (1987) 343–356.
[11] Y.H. Huang, A.E. Jakus, S.W. Jordan, et al., Three-dimensionally printed hyperelastic bone scaffolds accelerate bone regeneration in critical-size calvarial bone defects, Plast. Reconstr. Surg. 143 (2019).
[12] J. Visser, F. Melchels, J.E. Jeon, et al., Reinforcement of hydrogels using three-dimensionally printed microfibres, Nat. Commun. 6 (2015) 6933.
[13] B.B. Xu, J. Ye, F.Z. Yuan, et al., Advances of stem cell-Laden hydrogels with biomimetic microenvironment for osteochondral Repair[J], Front. Bioeng. Biotechnol. 8 (2020) 247.
[14] Y. Yang, Z. Chen, X. Song, et al., Biomimetic anisotropic reinforcement architectures by electrically assisted nanocomposite 3D printing, Adv. Mater. 29 (11) (2017) 1605750.
[15] B.M. Baker, R.L. Mauck, The effect of nanofiber alignment on the maturation of engineered meniscus constructs, Biomaterials 28 (11) (2007) 1967–1977.
[16] J. Mei, Y. Yu, Z. Wang, et al., Decellularization of rat kidneys to produce extracellular matrix scaffolds, Methods Mol. Biol. 1397 (2016) 53–63.
[17] J.J. Song, J.P. Guyette, S.E. Gilpin, et al., Regeneration and experimental orthotopic transplantation of a bioengineered kidney, Nat. Med. 19 (5) (2013) 646–651.
[18] C.H. Lee, S.A. Rodeo, L.A. Fortier, et al., Protein-releasing polymeric scaffolds induce fibrochondrocytic differentiation of endogenous cells for knee meniscus regeneration in sheep, Sci. Transl. Med. 6 (266) (2014) 266ra171.
[19] R. Sridharan, A.R. Cameron, D.J. Kelly, et al., Biomaterial based modulation of macrophage polarization: a review and suggested design principles, Mater. Today 18 (6) (2015) 313–325.
[20] R.E. Mirza, M.M. Fang, W.J. Ennis, et al., Blocking interleukin-1β induces a healing-associated wound macrophage phenotype and improves healing in type 2 diabetes, Diabetes 62 (7) (2013) 2579–2587.
[21] J.M. Anderson, A. Rodriguez, D.T. Chang, Foreign body reaction to biomaterials, Semin. Immunol. 20 (2) (2008) 86–100.
[22] Q. Xu, C. He, C. Xiao, et al., Reactive oxygen species (ROS) responsive polymers for biomedical applications, Macromol. Biosci. 16 (5) (2016) 635–646.
[23] Y. Zhu, R. Hoshi, S. Chen, et al., Sustained release of stromal cell derived factor-1 from an antioxidant thermoresponsive hydrogel enhances dermal wound healing in diabetes, J. Contr. Release 238 (2016) 114–122.
[24] R.M. Boehler, J.G. Graham, L.D. Shea, Tissue engineering tools for modulation of the immune response, Biotechniques 51 (4) (2011) 239–240.
[25] K.S. Washington, C.A. Bashur, Delivery of antioxidant and anti-inflammatory agents for tissue engineered vascular grafts, Front. Pharmacol. 8 (2017) 659.

[26] J.N. Fullerton, D.W. Gilroy, Resolution of inflammation: a new therapeutic frontier, Nat. Rev. Drug Discov. 15 (8) (2016) 551–567.
[27] Y.H. Yang, E. Morand, M. Leech, Annexin A1: potential for glucocorticoid sparing in RA, Nat. Rev. Rheumatol. 9 (10) (2013) 595–603.
[28] M. Perretti, N. Chiang, M. La, et al., Endogenous lipid- and peptide-derived anti-inflammatory pathways generated with glucocorticoid and aspirin treatment activate the lipoxin A4 receptor, Nat. Med. 8 (11) (2002) 1296–1302.
[29] M. Perretti, F. D'Acquisto, Annexin A1 and glucocorticoids as effectors of the resolution of inflammation, Nat. Rev. Immunol. 9 (1) (2009) 62–70.
[30] G. Fredman, N. Kamaly, S. Spolitu, et al., Targeted nanoparticles containing the proresolving peptide Ac2-26 protect against advanced atherosclerosis in hypercholesterolemic mice, Sci. Transl. Med. 7 (275) (2015), 275ra220.
[31] G. Leoni, P.A. Neumann, N. Kamaly, et al., Annexin A1-containing extracellular vesicles and polymeric nanoparticles promote epithelial wound repair, J. Clin. Investig. 125 (3) (2015) 1215–1227.
[32] Z.Z. Zhang, D. Jiang, J.X. Ding, et al., Role of scaffold mean pore size in meniscus regeneration, Acta Biomater. 43 (2016) 314–326.
[33] J. Li, J. Wang, Y. Zou, et al., The influence of delayed compressive stress on TGF-β1-induced chondrogenic differentiation of rat BMSCs through Smad-dependent and Smad-independent pathways, Biomaterials 33 (2012) 8395–8405.
[34] B.M. Baker, R.P. Shah, A.H. Huang, R.L. Mauck, Dynamic tensile loading improves the functional properties of mesenchymal stem cell-laden nanofiber-based fibrocartilage, Tissue Eng. 17 (2011) 1445–1455.
[35] A. Anna, C.C. José, J.A. María, Engineering anisotropic meniscus: zonal functionality and spatiotemporal drug delivery, Tissue Eng. B 27 (2) (2021) 133–153.
[36] B. Wang, A.J. Benitez, F. Lossada, et al., Bioinspired mechanical gradients in cellulose nanofibril/polymer nanopapers, Angew. Chem. Int. Ed. 55 (20) (2016) 5966–5970.
[37] S. Rhee, J.L. Puetzer, B.N. Mason, et al., 3D bioprinting of spatially heterogeneous collagen constructs for cartilage tissue engineering, ACS Biomater. Sci. Eng. 2 (10) (2016) 1800–1805.
[38] D. Kokkinis, F. Bouville, A.R. Studart, 3D printing of materials with tunable failure via bioinspired mechanical gradients, Adv. Mater. 30 (19) (2018) 1705808.
[39] A. Atala, S.B. Bauer, S. Soker, et al., Tissue-engineered autologous bladders for patients needing cystoplasty, Lancet 367 (2006) 1241–1246.
[40] J. Kajstura, M. Rota, S.R. Hall, et al., Evidence for human lung stem cells, N. Engl. J. Med. 364 (2011) 1795–1806.
[41] H.C. Ott, T.S. Matthiesen, S.K. Goh, et al., Perfusiondecellularized matrix: using nature's platform to engineer a bioartificial heart, Nat. Med. 14 (2008) 213–221.
[42] C.N. Serhan, N. Chiang, T.E. Van Dyke, Resolving inflammation: dual anti-in Flammatory and pro-resolution lipid mediators, Nat. Rev. Immunol. 8 (5) (2008) 349–361.
[43] A.C. Tiago, Z. Loannis, T. Alexandros, et al., Microalgal lipid extracts have potential to modulate the inflammatory response: a critical review, Int. J. Mol. Sci. 22 (18) (2021) 9825.
[44] N. Kamaly, G. Fredman, M. Subramanian, et al., Development and in vivo efficacy of targeted polymeric inflammation-resolving nanoparticles, Proceedings of the National Academy of Sciences of the United States of America 110 (16) (2013) 6506–6511.
[45] Pessolano Belvedere, Bizzarro, et al., Annexin A1 contained in extracellular vesicles promotes the activation of keratinocytes by mesoglycan effects: an autocrine loop through FPRs, Cells 8 (7) (2019) 753.
[46] C.Y. Ji, L.L. Lan, H.Y. Qing, et al., Targeted treatment of ischemic stroke by bioactive nanoparticle-derived reactive oxygen species responsive and inflammation-resolving nanotherapies, ACS Nano 15 (10) (2021) 16076–16094.
[47] C. Li, Y. Zhao, J. Cheng, et al., A proresolving peptide nanotherapy for site-specific treatment of inflammatory bowel disease by regulating proinflammatory microenvironment and gut microbiota, Adv. Sci. 6 (18) (2019) 1900610.
[48] N. Kamaly, G. Fredman, M. Subramanian, et al., Development and in vivo efficacy of targeted polymeric inflammation-resolving nanoparticles, Proceedings of the National Academy of Sciences of the United States of America 110 (16) (2013) 6506–6511.
[49] J.H. Jun, J.X. Chong, W. Ying, et al., Annexin A1-derived peptide Ac2-26 facilitates wound healing in diabetic mice, Wound Repair Regen. 28 (6) (2020) 772–779.
[50] R. Stefan, L.J. Hyun, M. Elias, et al., Ac2-26-nanoparticles induce resolution of intestinal inflammation and anastomotic healing via inhibition of NF-κB signaling in a model of perioperative colitis[J], Inflamm. Bowel Dis. 27 (9) (2021) 1379–1393.
[51] N. Fahy, M.L. de Vries-van Melle, J. Lehmann, et al., Human osteoarthritic synovium impacts chondrogenic differentiation of mesenchymal stem cells via macrophage polarisation state, Osteoarthritis Cartilage 22 (8) (2014) 1167–1175.